

# UC San Diego

## UC San Diego Previously Published Works

### Title

FGF signalling restricts haematopoietic stem cell specification via modulation of the BMP pathway

### Permalink

<https://escholarship.org/uc/item/6k00g2mx>

### Journal

Nature Communications, 5(1)

### ISSN

2041-1723

### Authors

Pouget, Claire  
Peterkin, Tessa  
Simões, Filipa Costa  
[et al.](#)

### Publication Date

2014

### DOI

10.1038/ncomms6588

Peer reviewed



# HHS Public Access

Author manuscript

*Nat Commun.* Author manuscript; available in PMC 2015 May 27.

Published in final edited form as:

*Nat Commun.* ; 5: 5588. doi:10.1038/ncomms6588.

## FGF signaling restricts hematopoietic stem cell specification via modulation of the BMP pathway

Claire Pouget<sup>1,2</sup>, Tessa Peterkin<sup>2</sup>, Filipa Costa Simões<sup>2,3</sup>, Yoonsung Lee<sup>1</sup>, David Traver<sup>1,\*</sup>, and Roger Patient<sup>2,\*</sup>

<sup>1</sup>Department of Cellular and Molecular Medicine and Section of Cell and Developmental Biology, University of California, San Diego, La Jolla CA 92093

<sup>2</sup>MRC Molecular Hematology Unit, Weatherall Institute of Molecular Medicine, University of Oxford, Oxford OX1 9DS, UK

### SUMMARY

Hematopoietic stem cells (HSCs) are produced during embryogenesis from the floor of the dorsal aorta. The localization of HSCs is dependent upon the presence of instructive signals on the ventral side of the vessel. The nature of the extrinsic molecular signals that control the aortic hematopoietic niche is currently poorly understood. Here we demonstrate a novel requirement for FGF signaling in the specification of aortic hemogenic endothelium. Our results demonstrate that FGF signaling normally acts to repress BMP activity in the subaortic mesenchyme through transcriptional inhibition of *bmp4*, as well as through activation of two BMP antagonists, *noggin2* and *gremlin1a*. Taken together, these findings demonstrate a key role for FGF signaling in establishment of the developmental HSC niche via its regulation of BMP activity in the subaortic mesenchyme. These results should help inform strategies to recapitulate the development of HSCs in vitro from pluripotent precursors.

### Keywords

FGF; BMP; stem cell; definitive blood; zebrafish

### INTRODUCTION

HSCs ultimately maintain all lineages of blood and immune cells throughout the lifetime of an organism. This feature underlies the long-term efficacy of bone marrow transplantation, frequently used as therapy for blood disorders including leukemia. Immune incompatibility between donor and host, insufficient number of donors, and the rarity of HSCs within many

---

Corresponding Author: Roger Patient, Tel: +44 1865 222613, Fax: +44 1865 222501, roger.patient@imm.ox.ac.uk. David Traver, Tel: +1 (858) 822-4593, Fax: +1 (858) 534-5457, dtraver@ucsd.edu.

<sup>3</sup>Present address: Department of Physiology, Anatomy and Genetics, University of Oxford, Oxford OX1 3QX, UK.

#### Author contributions

C.P. led the study, conducted the experiments, analyzed the data, and wrote the paper; T.P. and F.C.S. conducted experiments, analyzed the data, and edited the manuscript; Y.L. analyzed the data; D.T. and R.P. supervised the study and edited the manuscript.

#### Competing financial interests

The authors declare no competing financial interests

donor tissues have led to a search for alternative approaches to traditional HSC-based therapies. Recent breakthroughs using induced Pluripotent Stem Cells (iPSCs) have brought hope of *in vitro* derived, patient-specific HSCs, which could circumvent these issues. Despite decades of effort, it is not currently possible to generate *bona fide* HSCs from pluripotent precursors. The development of novel HSC-based therapeutics may thus depend upon obtaining a more precise understanding of the native molecular events that occur *in vivo* during HSC formation.

In all vertebrate animals examined, HSCs arise during embryogenesis from a specialized population of arterial cells localized in the ventral side of the dorsal aorta (DA) termed hemogenic endothelium<sup>1</sup>. This endothelial-hematopoietic transition<sup>2</sup> appears to exist only transiently, and is characterized by changes in gene expression and shape in ventral aortic endothelial cells as HSC precursors emerge and then enter circulation<sup>2-6</sup>. A prerequisite for HSC emergence appears to be the normal specification of arterial fate, most importantly proper formation of the DA. At the molecular level, arterial identity is governed by multiple extrinsic signals. In the zebrafish embryo, Hedgehog signals from the notochord/floor plate regulate the expression of *vegfa* and *calcitonin* in the somites, which in turn regulate expression of *Notch* receptors in the DA<sup>7-11</sup>. Modulation of any of these signaling pathways alters arterial development and therefore HSC formation.

Recent studies have demonstrated that HSC formation is disrupted by defects in the *Wnt16*<sup>12</sup>, *Vegfa*<sup>13</sup> and *Bmp4*<sup>14</sup> pathways without concomitant loss of aortic fate. Interestingly, each pathway regulates different steps of HSC development. In zebrafish, *Wnt16* controls early HSC specification through its regulation of the somitic Notch ligand genes *deltaC* and *deltaD*, whose combined action is required for the Notch-dependent specification of HSCs, but not for arterial development<sup>12</sup>. More recently, it was confirmed in *Xenopus* that arterial fate and HSC emergence can be uncoupled based on *Vegfa* isoforms. The short isoform controls arterial fate likely through *Notch4*, while HSC emergence depends on the medium/long isoforms and *Notch1*<sup>13</sup>. Finally, *Bmp4* that is localized to the sub-aortic mesenchyme is responsible for the polarization of HSC formation from the ventral side of the DA<sup>14-17</sup>. *Smad1*, an intracellular activator of the BMP pathway, transactivates the *runx1* promoter *in vitro*, suggesting that *Bmp4* may act directly upstream of *runx1*<sup>18</sup>, which is required for the emergence of HSCs across vertebrate species<sup>8,19-21</sup>. Just before the onset of definitive hematopoiesis in zebrafish, the aortic region switches from a BMP repressive to activated environment<sup>14</sup>. The mechanism of this sudden change remains unknown.

Interplay between BMP and FGF signaling pathways has been described during organogenesis. In *Xenopus*, FGF and BMP signaling pathways intersect in the regulation of primitive erythropoiesis where FGF inhibits *Bmp4*-induced erythropoiesis through the control of *gata2*<sup>22</sup>. The repressive role of FGF in primitive blood is conserved across the vertebrates. For instance, in the chicken embryo, FGF signals through *Fgfr2* to control erythrocyte differentiation by repressing *gata1* expression in blood precursors<sup>23</sup>. In *Xenopus*, FGF was shown to act on the timing of primitive hematopoiesis by holding back the onset of the molecular program that triggers primitive blood formation<sup>24</sup>. Finally, in zebrafish, primitive erythrocyte formation depends on *Fgf21*, which also governs

erythromyeloid precursor development, likely in concert with Fgf1<sup>23,25,26</sup>. While several studies have established that FGF signaling represses primitive blood formation, FGF signaling acts as a positive regulator of adult HSCs. Fgf1<sup>27</sup> and Fgf2<sup>28</sup> can expand *ex vivo* the number of transplantable HSCs. However, this effect seems to be limited to the short-term HSC compartment *in vivo* and it is accompanied by an alteration of the terminal differentiation of erythrocytes, B-cells and myeloid cells<sup>29</sup>. More recently, the role of FGF signaling in steady state conditions has been challenged and seems to be mainly required to promote mobilization and proliferation of HSCs under stress induced conditions<sup>30,31</sup>. FGF signaling appears to have multiple roles in blood development, however, its potential role in the emergence of HSCs has not been addressed.

In this study, we have discovered a key repressive role for FGF signaling in HSC emergence through its regulation of the BMP pathway. Together with the data in the accompanying paper (Lee et al), which reveals an earlier positive role for FGF in programming the HSC lineage, these findings suggest that precise temporal inhibition as well as activation of FGF signaling may aid *in vitro* approaches to instruct HSC fate from pluripotent precursors.

## RESULTS

### FGF signaling is a negative regulator of HSC formation in the zebrafish embryo

To functionally test whether or not FGF signaling is required for definitive blood formation, we utilized transgenic zebrafish in which FGF signaling can be inducibly abrogated or enforced by heat-shock induction of a dominant-negative Fgfr1-EGFP fusion protein (*hsp70:dn-fgfr1-EGFP*)<sup>32,33</sup>, or a constitutively active Fgfr1 mutant protein (*hsp70:ca-fgfr1*)<sup>34</sup>, respectively. This time controlled approach allowed us to avoid mesoderm patterning defects induced by early FGF misexpression and subsequently target different developmental events according to their timing<sup>35</sup>.

In order to identify temporal windows when FGF signaling may be involved in HSC development, we initially targeted the early stage of arterial specification by inducing the *hsp:dn-fgfr1* transgene at 17 hpf (15 somite stage (ss)). At this stage, primitive blood and endothelial cells are specified and the first sign of arterial specification is detectable in the endothelial precursors that are migrating from the lateral plate mesoderm to the midline<sup>36</sup> to form the primitive vascular cord<sup>37-39</sup>. Transgenic embryos were then sorted based on the expression of GFP, and GFP negative embryos were used as sibling controls. Following induction of *hsp:dn-fgfr1*, definitive hematopoiesis initiated normally and there was no significant difference in *runx1* expression between GFP+ and GFP- animals (Supplemental Fig. 1A and B). Interestingly, arterial and endothelial differentiation were unaffected, based upon the normal expression of *deltaC* and *kdrl*, respectively (Supplemental Fig. 1C-F), suggesting that FGF signaling is not required for arterial differentiation or vascular development during the convergence of vascular precursor cells to the midline.

To investigate possible later requirements for FGF signaling in HSC development, embryos were heat-shocked at 20.5 hpf (23 ss), just prior to when *runx1* expression along the aortic floor marks initiation of the definitive HSC program. To verify loss of FGF signaling, we analyzed the expression of *pea3*, a direct transcriptional target<sup>40</sup> of FGF signaling. In

embryos heat-shocked at 20.5 hpf, *pea3* expression decreased, and was accompanied by an increase in *runx1* expression (Figure 1, A, B and D, E). At the stage when the heatshock was performed, the aortic region contains the precursors of the HSCs that will specifically express *runx1* from 23hpf, but also primitive blood that can be distinguished from HSC based on *gata1* expression. The effect of the modulation of FGF signaling is restricted to the HSCs as shown by the absence of alteration of *gata1* expression in transgenic embryos (Supplemental Fig. 2 A). EMPs, bipotent precursors that arise in the posterior blood island<sup>41</sup>, are not affected upon FGF modulation (Supplemental Fig. 2 A). In converse experiments, where FGF signaling was enforced via 20.5 hpf induction of the *hsp:ca-fgfl* transgene, embryos exhibited embryo-wide upregulation of *pea3* expression and a substantial decrease in *runx1* expression along the aortic floor (Figure 1, C and F). Despite strong GFP expression at 5 hours post-heatshock (hpHS), *hsp:dn-fgfr1* embryos displayed only a slight decrease in *pea3* expression, leading to the conclusion that cellular turnover of the truncated receptor may outpace the turnover of GFP. To address this, *pea3* expression was analyzed in *hsp:dn-fgfr1* embryos from 23 hpf to 27 hpf. At 2 hpHS, *pea3* was nearly absent in GFP+ embryos. Expression of *pea3* gradually returned to normal around 6 hpHS (Supplemental Fig. 2 B). Effects on *runx1* expression followed this trend. Between 2–4 hpHS a greater proportion of *hsp:dn-fgfr1* embryos showed stronger upregulation of *runx1* than when analyzed between 5–6 hpHS (Supplemental Fig. 2C). The effects of Fgf modulation on *runx1* expression were confirmed by quantitative PCR using cDNAs from the dissected trunks of *hsp:dn-fgfr1* and *hsp:ca-fgfr1* embryos (Figure 1G).

Before 26–27 hpf, the close proximity of primitive erythrocytes within the DA and posterior cardinal vein (PCV) to the floor of the DA<sup>42</sup> makes it difficult to distinguish them from emerging HSCs since each lineage shares expression of early hematopoietic markers. We therefore shifted the heat-shock regimen to 25 hpf and fixed at 30 hpf. By this time, erythroid precursors have entered circulation, which allows visualization of the hemogenic endothelial markers *cmyb* by whole-mount in situ hybridization (WISH). Induced *hsp70:dn-fgfr1* embryos showed elevated expression of both *runx1* and *cmyb* in the DA (Figure 1 H–K, Supplemental Fig. 2 D) within the period during which the FGF transcriptional target *pea3* is still downregulated (Figure 1 L and M). In mammals, HSCs leave the DA region quickly after their emergence to seed the fetal liver and the thymus. In zebrafish, a similar shift occurs: *runx1*+/*cmyb*+ cells migrate from the DA to the caudal hematopoietic tissue (CHT) and the thymus<sup>43–45</sup>. To ascertain whether the expanded pool of *runx1*+/*cmyb*+ cells are HSCs, FGF signaling was modulated at 25hpf and the effect on HSCs was monitored in the DA, the CHT and the thymus at 36hpf (25hpf + 12h), 3 (25hpf + 48h), and 4dpf (25hpf + 72h)(Fig. 1. O–W, Supplemental Fig. 2 E and F). In induced *hsp70:dn-fgfr1* embryos, *cmyb* expression is still expanded in the DA 12hpHS (Fig. 1 O and P). Conversely, embryos in which FGF signaling was enforced are devoid of *cmyb* cells in the DA (Fig. 1 O and Q). Similarly, at 48 and 72hpHS, *hsp70:dn-fgfr1* embryos showed a more robust expression of *runx1* and *cmyb* in the CHT while *hsp70:ca-fgfr1* embryos showed a drastic decrease of the *runx1*+ and *cmyb*+ cells (Supplemental Fig. 2 E, Fig. 1 R–T). Quantitative PCR analysis of dissected CHT confirmed that *runx1*, *cmyb* and *CD41* levels of expression vary according to the modulation of FGF signaling (Supplemental Fig. 2 F). T-cells are thought to be the first functional derivatives of HSCs. They are first detected around 3 dpf

and by day4, *rag1* expression becomes robust in the thymus. The effect of FGF signaling modulation at 25hpf also affects the number of thymic *rag1*<sup>+</sup> (Fig. 1 U–W). Importantly, the increase in the number of *rag1*<sup>+</sup> cells was observed only in *hsp70:dn-fgfr1* embryos whose blood circulation was unaffected.

Taken together, these results demonstrate that FGF signaling is important in the establishment of hemogenic endothelium, acting to repress the specification of HSC fate from the aortic floor.

### **Fgf10a represses HSC formation possibly by acting on fgfr2 and fgfr3**

To identify the cell types that may mediate the effects of FGF signaling on HSC emergence, we examined localization of Fgf receptor expression at 20.5 hpf and at 24 hpf (Supplemental Fig. 3). *Fgfr1a*, *fgfr 1b*, and *fgfr 4* were not detected in the tissues surrounding the DA at either time point (Supplemental Fig. 3 A–H and Q–T). *Fgfr2* showed strong expression in the pronephric ducts, the hypochord, and the neural tube at 20.5 hpf (Supplemental Fig. 3I and J). In contrast to *fgfr2*, *fgfr3* transcripts were detected in the somites at 20.5 hpf (Supplemental Fig. 3 M and N). At 24 hpf, *fgfr3* is expressed throughout the trunk, whereas *fgfr2* expression is restricted to the neural tube, the pronephric ducts, the hypochord, and in cells surrounding the axial vasculature (Supplemental Fig. 3K, L and O, P). The localization of each receptor suggests that the effects of FGF modulation on HSC formation may act through *fgfr2* and/or *fgfr3*. However, morpholino knockdown of these receptors failed to phenocopy the increase in *runx1* and *cmyb* expression observed in the *hsp70:dn-fgfr1* transgenic line. Loss of either receptor led to the absence of *runx1* expression in the DA at 26 hpf (Supplemental Fig. 4). The discrepancy between the phenotype observed in morphants and that observed in *hsp70:dn-fgfr1* embryos suggests that *fgfr2* and *fgfr3* may be required at earlier stages of mesoderm or vascular development.

In zebrafish, 27 Fgf ligands have been identified<sup>46</sup>. At the stage of the heatshock, *fgf10a* is expressed throughout the trunk<sup>47</sup> which made it a good candidate. To analyze its potential role in HSC specification, knockdown experiments were carried out using a splice-blocking morpholino (Figure 2). Our LOF experiments showed that depletion of *fgf10a* gives a similar phenotype than the phenotype observed in the *hsp70:dn-fgfr1* embryos. At 30hpf, in morphant embryos, *runx1* and *cmyb* expression are extended along the entire DA (Figure 2 A–D and E).

Taken together, our results confirm that FGF signaling acts as a negative regulator of definitive hematopoiesis. This function is mediated by *fgf10a* which likely signals through *fgfr2* and/or *fgfr3*.

### **FGF acts independently of the Notch and Vegf pathways**

In both mouse and zebrafish, Notch signaling is required for aortic and HSC specification<sup>9,21,48,49</sup>. Since *fgfr2* is expressed in the aortic region and *fgfr3* in the somites, it is possible that the effects of FGF signaling on HSC emergence could be due in part to effects on the Notch pathway. In zebrafish, enforced expression of the Notch intra cellular domain (NICD) throughout the embryo is sufficient to generate an excess of HSCs<sup>21</sup>.

Similarly in mice, genetic depletion of COUP-TFII, which normally represses Notch in the PCV, leads to the formation of ectopic hematopoietic clusters in the PCV<sup>50</sup>. We therefore investigated whether the modulation of HSC number observed in the DA following loss or gain of FGF signaling might be due to effects on the Notch pathway. Transgenic *hsp70:dn-fgfr1* or *hsp70:ca-fgfr1* embryos were heatshocked at 20.5 hpf, fixed at 25 hpf, then assayed for Notch-related vascular and arterial gene markers by WISH (Supplemental Fig. 5 A–O). Following either loss or gain of FGF function, the integrity of the vascular system was unaffected, as indicated by normal *kdrl* expression (Supplemental Fig. 5 A–C). Aortic markers, including *gridlock* (a target of the Vegf pathway<sup>9</sup>) (Supplemental Fig. 3 D–F), *notch1b* (Supplemental Fig. 5 G–I), *deltaC* (Supplemental Fig. 5 J–L), and *ephrinb2a* (a target of the Notch pathway<sup>48</sup>) (Supplemental Fig. 5 M–O) were unchanged following modulation of FGF signaling. These results indicate that the effects of FGF signaling on HSC fate are not dependent upon downstream Notch signaling events. To test the converse, that is whether or not FGF signaling requirements are downstream of Notch, Notch signaling was blocked using DAPM, a small chemical inhibitor of NICD release from Notch receptors. If the increase in HSC number following FGF inhibition acts downstream of Notch, blockade of Notch signaling in the same temporal window as FGF inhibition should not prevent *runx1* upregulation in the DA. In accord with this hypothesis, *hsp70:dn-fgfr1* embryos treated with DAPM maintained strong expression of *runx1* in the DA (Supplemental Fig. 5 P–U). These results demonstrate that the increase in HSC number observed in absence of FGF signaling acts in a dominant manner with respect to loss of Notch signaling. Taken together, our studies on the interaction of Notch and FGF suggest that the effects of FGF on HSC fate either occur independently or downstream of the roles of the Notch/Vegf signaling axis during arterial development and HSC formation.

### FGF signaling does not affect dorsal polarization of the DA

Since the increase in HSC marker expression in the DA is not a result of overactivation of the Vegf or Notch signaling pathways, we reasoned that it may be due to an increase in the number of *runx1*<sup>+</sup> cells in the DA or the surrounding mesenchyme. We thus examined *runx1* expression in transverse sections following induction of the *hsp70:dn-fgfr1* transgene at 20.5 hpf. In WT controls, rare *runx1*<sup>+</sup> cells were visible only in the floor of the DA (Figure 3 A–C). Following loss of FGF signaling, the expression of *runx1* in the DA was expanded beyond the floor region to the roof of the aorta (Figure 3 D–E). Cells expressing *runx1* were never detected in the surrounding mesenchyme or neighboring PCV, suggesting that ectopic *runx1*<sup>+</sup> cells must transit through an arterial precursor. Since *runx1* is normally expressed only in the aortic floor, the ectopic appearance of *runx1*<sup>+</sup> cells in the aortic roof may indicate that FGF signaling is involved in DA polarization. In mice and zebrafish, DA polarization depends upon opposing morphogen gradients; dorsal identity is established by Hedgehog secretion from the notochord whereas ventral identity relies upon BMP production from ventral domains<sup>14–16</sup>. We examined the expression of *tbx20*, a transcription factor regulated by Hedgehog signaling<sup>8,14,51</sup>, that distinguishes the dorsal side of the DA. Neither activation nor inhibition of FGF signaling had any effect on *tbx20* expression (Figure 3 F, H and J). Examination of transverse sections confirmed that only cells in the roof of the DA and in the developing intersomitic vessels expressed *tbx20*,

indicating that dorsal polarization is not affected by FGF modulation (Figure 3 G, I, K and L).

### FGF signaling controls HSC formation by modulating BMP activity

We next investigated whether FGF regulates the ventral polarization of the DA by modulating BMP activity. In zebrafish, we previously demonstrated that *bmp4* is required for the emergence and maintenance of HSCs<sup>14</sup>. Whereas *bmp4* is normally expressed in the mesenchyme underlying the DA (Figure 4A, D and G), *bmp4* expression was upregulated in the aortic region in the absence of FGF (Figure 4B, E and H). Conversely, in embryos with FGF overactivation, *bmp4* was absent from the aortic region (Figure 4C, F and I), supporting the idea that FGF signaling may regulate HSC formation via its effects on the BMP pathway.

Since BMP signaling activity is tightly regulated by several antagonists<sup>52</sup>, we also examined their expression at the time of heat shock. At 20.5 hpf, the DA is surrounded by several BMP antagonists, including *chordin* from the pronephric ducts, as well as *noggin1*, *noggin2*<sup>53</sup>, and *gremlin1a*<sup>54</sup>. Although *chordin* is an important regulator of primitive hematopoiesis<sup>55</sup>, it is dispensable for HSC formation<sup>14</sup>. We therefore focused on *noggin1*, *noggin2*, and *gremlin1a*. In WT embryos, *noggin1* is barely detected in the ventral side of the somite at 24hpf, while *gremlin1a* and *noggin2* are strongly expressed in the sclerotome (Figure 4J, M)<sup>53,54</sup>. In induced *hsp70:dn-fgfr1* embryos, both *gremlin1a* and *noggin2* were markedly downregulated (Figure 4K, N and Supplemental Fig. 6). In contrast, when FGF signaling was enforced there was substantial upregulation of sclerotomal *gremlin1a* and *noggin2* (Figure 4L, O and Supplemental Fig. 6). Augmentation of FGF activity was also observed to induce ectopic expression of *gremlin1a* and *noggin2* in the most dorsal compartment of the somite (Figure 4L, O). Together, these results demonstrate that FGF signaling represses *bmp4* expression directly, and concomitantly induces expression of the BMP inhibitors *noggin2* and *gremlin1a* in the neighboring somite.

To further analyze how FGF and BMP signaling interact, we tested whether inhibition of BMP signaling in FGF depleted embryos would affect *runx1* expression. Inhibition of FGF signaling, either using the *hsp:dn-fgfr1* transgenic animals or a small chemical inhibitor su5402, increases *runx1* expression in the DA (Figure 5A, B, C), while blockage of BMP signaling abrogates *runx1* expression (Figure 5D). Inhibition of FGF signaling in a BMP-repressed environment could not rescue HSC production, supporting the idea that FGF acts upstream of the BMP pathway (Figure 5E).

To further examine the epistasis between the FGF and BMP pathways, we sought a molecular marker of BMP activity. The transcriptional repressor *idl* is a known target of BMP signaling<sup>56</sup>, and its targeted deletion in the mouse embryo impairs hematopoiesis by affecting the proliferation and the self-renewal of HSCs<sup>57</sup>. In zebrafish, *idl* is expressed in developing neural tissue, somites and axial vasculature (Figure 5F); this expression is largely ablated following inhibition of BMP signaling (Figure 5G). Inhibition of FGF signaling leads to an increase in *idl* expression in the vasculature (Figure 5 F, H), which becomes more apparent in transverse sections (Figure 5 J, K). Conversely, stimulation of FGF significantly decreases *idl* expression (Figure 5 I). Together, these results further



demonstrate that the FGF signaling pathway acts upstream of BMP signaling to regulate HSC emergence.

Finally, we performed genetic rescue experiments to determine if enforced BMP signaling could rescue loss of HSCs in *hsp70:ca-fgfr1* animals. Enforced activity of the BMP pathway was achieved following induction of a constitutively active bmp receptor 1b (*hse:ca-bmpr1b*) construct in transient transgenic animals, as previously described<sup>58</sup>. Compared to WT siblings, *hsp70:ca-fgfr1* animals induced at 20.5 hpf showed loss of HSCs accompanied by an increase of *pea3* expression (Figure 6A, B and E). Induction of the *hse:ca-bmpr1b* transgene alone showed a robust increase in *runx1* expression without affecting *pea3* (Figure 6C and E). As predicted by our results above, enforced activity of BMP signaling could rescue HSC development in *hsp70:ca-fgfr1* animals (Figure 6D and E).

In this experiment, BMP signaling was enforced at the receptor level, bypassing therefore any potential effect of the Bmp antagonists *noggin2* and *gremlin1a*. In *hsp:ca-fgfr1* embryos, their expression levels are elevated suggesting that they may reinforce the BMP repressive environment in the DA. According to this hypothesis, overexpression of *noggin2* or *gremlin1a* following inhibition of FGF signaling should prevent *runx1* increase. Overexpression of *noggin2* and *gremlin1a* were achieved by mRNA injection into *hsp70:dn-fgfr1* embryos and analyzed for *runx1* expression. As predicted, both *noggin2* and *gremlin1a* represses HSC formation when injected in control embryos (Figure 6. F, H and J). Similar results were obtained when *noggin2* and *gremlin1a* were overexpressed in *hsp:dn-fgfr1* embryos (Figure 6. G, I and K), confirming that both antagonists are acting downstream of FGF signaling and upstream of *bmp4/bmpr1*.

Collectively, our results indicate that FGF signaling controls the emergence of HSCs by modulating the activity of BMP signaling in the aortic region. The inhibition of BMP signaling by FGF acts at two levels, first by repressing the transcription of *bmp4* in the subaortic mesenchyme, and second by increasing the expression of BMP antagonists in the neighboring somite. These results suggest that the level of FGF signaling controls the capacity of the aortic microenvironment to support or repress the formation of HSCs (Figure 7).

## DISCUSSION

Despite FGF signaling playing key roles in the formation of mesoderm and the vascular system, no previous studies have examined potential roles for FGF in HSC development. Studies in adult mice have demonstrated that HSCs express *Fgfr1*, and that provision of *Fgf1* *ex vivo* can stimulate HSC expansion<sup>27</sup>. More recent work, however, has demonstrated that *Fgfr1* is not required for the normal homeostasis of adult HSCs, but rather in hematopoietic recovery following injury via irradiation or chemotherapy by stimulating HSC proliferation<sup>30</sup>. FGF signaling may therefore be important in regulating the number of adult HSCs.

A current bottleneck in the field of regenerative medicine is the inability to instruct HSC fate *in vitro* from pluripotent precursors, including iPSCs. This is due, at least in part, to an

incomplete understanding of the native factors that are required to specify HSCs during embryonic development. In this study, we have demonstrated a novel requirement for FGF signaling in the generation of HSCs. We show that FGF represses the emergence and maintenance of HSCs in the DA by blocking BMP signals that originate from the aortic mesenchyme. This negative role is in contrast to the role that FGF signaling has in adult hematopoiesis, where it promotes HSC amplification. Along with the results of the companion paper (Lee et al.), it is now apparent that the FGF pathway is required at multiple stages of development to properly specify HSC fate.

HSCs originate from arterial precursors, which depend upon the Notch and Vegf signaling pathways for their specification and differentiation<sup>7,9,11,21,48,49,59</sup>. Unlike the results of Lee et al., where early FGF signaling (14–17 hpf) is required within the somite to bridge the Wnt16-mediated expression of the Notch ligand *deltaC*, the subsequent FGF signaling requirement (22–30 hpf) for HSC emergence lies downstream of Notch function. Neither Notch nor Vegf dependent gene expression programs were affected following modulation of FGF activity after 20.5 hpf. Moreover, the combined inhibition of Notch and FGF signaling failed to decrease *runx1* expression in the DA, indicating that FGF acts downstream of the Notch pathway in HSC emergence. Interestingly, while FGF inhibition increased the number of HSCs emerging from the DA, we did not observe ectopic *runx1*<sup>+</sup> cells outside of the DA, suggesting that FGF signaling affects only arterial precursors previously specified by Notch signaling.

Following the induced repression of FGF signaling, *runx1* expression expands dorsally within the DA without affecting dorsal identity, as defined by the normal expression of *tbx20*. This finding suggests that the expression domains of *runx1* and *tbx20* are not mutually exclusive, confirming our previous report<sup>14</sup>. Interestingly, the expanded pool of *runx1*+/*cmlyb*+ cells behave as normal HSC. Ectopically induced HSCs have the capacity to migrate from the DA, seed the different hematopoietic organs, and differentiate into T-cells in the embryos showing normal blood flow 2 to 3 days after heatshock.

The proper establishment of ventral aortic identity, in contrast to the dorsal identity, appears to depend upon the FGF pathway. FGF signaling controls the ventral polarization of the DA by restricting *bmp4* expression in the mesenchyme around the aortic endothelium. The timing and location of *bmp4* expression in the sub-aortic mesenchyme is conserved among several classes of vertebrates<sup>14,15,17,60</sup>. Interestingly, clusters of blood cells emerge from both the dorsal and ventral side of the DA in mouse embryos<sup>61</sup>. However, the adult reconstituting potential is restricted to the ventral clusters<sup>62</sup>, supporting the idea that the ventral mesenchyme provides the cues critical to conferring stem cell potential. This hypothesis is supported by previous findings, where early resection of ventral mesenchyme led to loss of aortic *runx1* expression and hematopoietic cluster formation<sup>3</sup>. Our analysis of *fgfr2* and *fgfr3* expression patterns showed that while *fgfr3* is mainly found in the somitic tissue at the time of HSC emergence, *fgfr2* transcripts are detected in the few cells surrounding the axial vasculature corresponding to the territory of expression of *bmp4*. This tissue localization suggests that *fgfr2* may mediate the effect observed on *bmp4* expression when FGF signaling is modulated. Fgf10a, whose loss gives rise to a similar hematopoietic phenotype to that observed in the *hsp:dn-fgfr1*, was shown to preferentially interact with

*fgfr2*<sup>63</sup>, supporting the existence of an axis involving *fgf10a/fgfr2/bmp4* to play the role of a switch that triggers the aortic blood program. However we cannot rule out that other Fgf ligands may be involved in the regulation of HSC specification from the hemogenic endothelium.

Our attempts to mimic the *hsp70:dn-fgfr1* phenotype by knocking down *fgfr2* and *fgfr3* failed and morphant embryos showed a drastic decrease of *runx1* expression at 26hpf. Knowing that Fgf receptors can heterodimerise<sup>64</sup> and that both *fgfr2* and *fgfr3* are expressed early on in the forming somites<sup>65,66</sup>, it is possible that *fgfr2* and *fgfr3* may be required in the somites to promote HSC specification in concert with *fgfr1* and *fgfr4*. To better understand how and when each receptor mediates the activity of the FGF signaling, new tools offering time control and tissue specificity have to be developed.

Our previous studies demonstrated that *bmp4* is crucial for HSC formation in zebrafish<sup>14</sup>. Attempts to locally increase Bmp4 activity using the zebrafish mutant in *chordin*, a Bmp antagonist, failed to increase *runx1* expression in the DA<sup>14</sup>, suggesting that *bmp4* alone is insufficient for HSC formation, or that other Bmp antagonists regulate HSC emergence. Our current findings indicate that the regulation of BMP signaling by FGF acts at multiple levels. First, enforced expression of a constitutively active Bmp receptor1 rescued *runx1* expression in *hsp70:ca-fgfr1* embryos, indicating that BMP signaling is sufficient to trigger the definitive hematopoietic program in the DA. This result, along with the finding that combined inhibition of FGF and BMP failed to generate HSCs, indicates that FGF signaling acts genetically upstream of BMP. In addition, inhibition of FGF function substantially increases *bmp4* expression in the subaortic mesenchyme and prevents expression of two BMP antagonists, *noggin2* and *gremlin1a*, in the surrounding somites. Here we report that overexpression of either *noggin2* or *gremlin1a* is enough to prevent *runx1* upregulation in the absence of FGF. This indicates that local increases of *bmp4* should be accompanied by inhibition of the *bmp4* antagonists, *gremlin1a* and *noggin2*, to trigger the definitive blood program. Collectively, these results indicate that ablation of FGF signaling intensifies the effects of BMP signaling in the DA on the hematopoietic program by both enhancing the expression of Bmp4 directly and repressing the expression of local BMP antagonists.

In conclusion, we show that the FGF signaling pathway is a negative regulator of HSC emergence through its control of *bmp4* function underlying the aortic floor. FGF signaling may thus provide a missing link in what regulates the developmental switch from a BMP repressive to supportive environment that is linked to the emergence of HSCs from ventral aortic endothelium. These findings suggest that careful modulation of the FGF/BMP signaling axis may be important in the instruction of HSC fate in regenerative medicine approaches.

## EXPERIMENTAL PROCEDURES

### Zebrafish strains

Wild type AB\* and transgenic lines, *hsp70:dn-fgfr1* (*Tg(hsp70l:dnfgfr-EGFP)<sup>pd1</sup>*)<sup>33</sup>, *hsp70:ca-fgfr1* (*Tg(hsp70l:Xla.fgfr1, cryaa:DsRed)<sup>pd3</sup>*)<sup>34</sup> and *hsp70:dn-bmpr1* (*tg(hsp70l:dn-bmpr1-EGFP)*)<sup>67</sup>, were maintained and stage as previously described in<sup>68</sup>. All

animal work was carried out according to UK Home Office and UCSD IACUC regulations and the under the appropriate project license.

### Heatshock conditions

Embryos were heatshocked by transferring them into prewarm E3 medium for 30 mins at either 39°C for *hsp70:dn-fgfr1*, *hsp70:ca-fgfr1*, *hsp70:ca-fgfr1* injected with *HSE:ca-bmpr1b-EGFP* construct<sup>58</sup> or 43°C for *hsp70:dn-bmpr1* then transferred to 28°C until fixation. Transgenic embryos were selected based on their reporter expression or by genotyping as previously described in<sup>69</sup>.

### Chemical treatments

Small molecule inhibitors were resuspended in DMSO and diluted in E3 medium. Su5402 (Calbiochem) was used at 5µM, and DAPM (Calbiochem) at 100µM<sup>70</sup>. Control embryos were treated with the corresponding volumes of DMSO added to E3 medium just after heatshock.

### WISH

Embryos were fixed in fresh PFA4%, dehydrated in EtOH and assayed for WISH as described in<sup>8</sup>. RNA probes were labelled with Digoxigenin (Roche) and detected using an anti-Dig antibody (Roche). Embryos were stained using a solution of NBT/BCIP (Roche).

### Wax sectioning

Embryos were dehydrated in EtOH 100% O/N, transferred in Xylene for 30mins then embedded in wax. Blocks containing stained embryos were sectioned at 10 or 4 µm using a microtome (Leica). Sections were transferred on glass slides, incubated at 37°C O/N. Wax was removed in xylene, and EtOH 100%, 70%, 50% and rehydrated in PBS. Slides were mounted and imaged. For the FGF receptors, representative embryos were selected and transversally sectioned using a razor blade. Slices of embryo were then soaked in glycerol and imaged.

### Transient transgenesis and injection experiments

20pg of *HSE:ca-bmpr1b-EGFP* transgenesis construct<sup>58</sup> combined to 25pg of transposase mRNA were injected in one cell stage of AB\* or *hsp70:ca-fgfr1* embryos. As a negative control, the construct was injected without transposase.

One-cell stage embryos were injected with morpholino solution diluted in water. Injected and uninjected embryos were incubated at 28°C until fixation. Sequences and working concentrations available in Supplemental Table 1.

### Real Time PCR

Total RNA was isolated from dissected trunk embryos, 5h after heat shock using the RNAeasy Micro Kit (Qiagen). Single heads of *hsp70:ca-fgfr1* were used for genotyping while corresponding trunks were kept individually on dry ice. Positive trunks were then pooled and processed as other samples with Superscript III Reverse Transcriptase

(Invitrogen). qPCR were performed with Sybr Green (Applied Biosystems) and analyzed by the comparative method ( $\Delta\Delta C_t$ ) with *efla* house-keeping gene as internal control. Statistical analysis was performed using t-test. Primer sequences available in Supplemental Table 1.

### Statistical analysis

All the experiments presented in this study were performed at least three times. Data were collected from independent experiments and are given as the mean  $\pm$  s.d. Student's t-test was used for statistical comparisons and  $p < 0.05$  were considered statistically significant.

### Supplementary Material

Refer to Web version on PubMed Central for supplementary material.

### Acknowledgments

We are grateful to D. Kimelman and K. Poss for sharing transgenic lines and the *hse:ca-bmpr1b-EGFP* transgenesis construct. We thank L. Zon, P. Crozier, I. Kobayashi, S. Wilson, M. Tada and K. Yamasu for sharing in situ probes. We are grateful to Emerald Butko and Maggie Walmsley for critical reading of the manuscript. This work was supported by the UK Medical Research Council (R.P) and the National Institutes of Health (D.T).

### References

- Swiers G, Rode C, Azzoni E, de Bruijn MF. A short history of hemogenic endothelium. *Blood cells, molecules & diseases*. 2013; 51:206–212.10.1016/j.bcmd.2013.09.005
- Kissa K, Herbomel P. Blood stem cells emerge from aortic endothelium by a novel type of cell transition. *Nature*. 2010; 464:112–115.10.1038/nature08761 [PubMed: 20154732]
- Richard C, et al. Endothelio-mesenchymal interaction controls runx1 expression and modulates the notch pathway to initiate aortic hematopoiesis. *Dev Cell*. 2013; 24:600–611.10.1016/j.devcel.2013.02.011 [PubMed: 23537631]
- Jaffredo T, Gautier R, Eichmann A, Dieterlen-Lievre F. Intraaortic hemopoietic cells are derived from endothelial cells during ontogeny. *Development*. 1998; 125:4575–4583. [PubMed: 9778515]
- Bertrand JY, et al. Haematopoietic stem cells derive directly from aortic endothelium during development. *Nature*. 2010; 464:108–111.10.1038/nature08738 [PubMed: 20154733]
- Boisset JC, et al. In vivo imaging of haematopoietic cells emerging from the mouse aortic endothelium. *Nature*. 2010; 464:116–120.10.1038/nature08764 [PubMed: 20154729]
- Lawson ND, Vogel AM, Weinstein BM. sonic hedgehog and vascular endothelial growth factor act upstream of the Notch pathway during arterial endothelial differentiation. *Dev Cell*. 2002; 3:127–136. [PubMed: 12110173]
- Gering M, Patient R. Hedgehog signaling is required for adult blood stem cell formation in zebrafish embryos. *Dev Cell*. 2005; 8:389–400.10.1016/j.devcel.2005.01.010 [PubMed: 15737934]
- Rowlinson JM, Gering M. Hey2 acts upstream of Notch in hematopoietic stem cell specification in zebrafish embryos. *Blood*. 2010; 116:2046–2056.10.1182/blood-2009-11-252635 [PubMed: 20511544]
- Nicoli S, Tobia C, Gualandi L, De Sena G, Presta M. Calcitonin receptor-like receptor guides arterial differentiation in zebrafish. *Blood*. 2008; 111:4965–4972.10.1182/blood-2007-10-118166 [PubMed: 18326814]
- Wilkinson RN, et al. Hedgehog signaling via a calcitonin receptor-like receptor can induce arterial differentiation independently of VEGF signaling in zebrafish. *Blood*. 2012; 120:477–488.10.1182/blood-2011-10-383729 [PubMed: 22668851]
- Clements WK, et al. A somitic Wnt16/Notch pathway specifies haematopoietic stem cells. *Nature*. 2011; 474:220–224.10.1038/nature10107 [PubMed: 21654806]

13. Leung A, et al. Uncoupling VEGFA functions in arteriogenesis and hematopoietic stem cell specification. *Dev Cell*. 2013; 24:144–158.10.1016/j.devcel.2012.12.004 [PubMed: 23318133]
14. Wilkinson RN, et al. Hedgehog and Bmp polarize hematopoietic stem cell emergence in the zebrafish dorsal aorta. *Dev Cell*. 2009; 16:909–916.10.1016/j.devcel.2009.04.014 [PubMed: 19531361]
15. Durand C, et al. Embryonic stromal clones reveal developmental regulators of definitive hematopoietic stem cells. *Proceedings of the National Academy of Sciences of the United States of America*. 2007; 104:20838–20843.10.1073/pnas.0706923105 [PubMed: 18087045]
16. Peeters M, et al. Ventral embryonic tissues and Hedgehog proteins induce early AGM hematopoietic stem cell development. *Development*. 2009; 136:2613–2621.10.1242/dev.034728 [PubMed: 19570846]
17. Suonpaa P, et al. Development of early PCLP1-expressing haematopoietic cells within the avian dorsal aorta. *Scandinavian journal of immunology*. 2005; 62:218–223.10.1111/j.1365-3083.2005.01655.x [PubMed: 16179008]
18. Pimanda JE, et al. The SCL transcriptional network and BMP signaling pathway interact to regulate RUNX1 activity. *Proceedings of the National Academy of Sciences of the United States of America*. 2007; 104:840–845.10.1073/pnas.0607196104 [PubMed: 17213321]
19. Okuda T, van Deursen J, Hiebert SW, Grosveld G, Downing JR. AML1, the target of multiple chromosomal translocations in human leukemia, is essential for normal fetal liver hematopoiesis. *Cell*. 1996; 84:321–330. [PubMed: 8565077]
20. North T, et al. Cbfa2 is required for the formation of intra-aortic hematopoietic clusters. *Development*. 1999; 126:2563–2575. [PubMed: 10226014]
21. Burns CE, Traver D, Mayhall E, Shepard JL, Zon LI. Hematopoietic stem cell fate is established by the Notch-Runx pathway. *Genes & development*. 2005; 19:2331–2342.10.1101/gad.1337005 [PubMed: 16166372]
22. Xu RH, et al. Opposite effects of FGF and BMP-4 on embryonic blood formation: roles of PV.1 and GATA-2. *Developmental biology*. 1999; 208:352–361. [PubMed: 10191050]
23. Nakazawa F, Nagai H, Shin M, Sheng G. Negative regulation of primitive hematopoiesis by the FGF signaling pathway. *Blood*. 2006; 108:3335–3343.10.1182/blood-2006-05-021386 [PubMed: 16888091]
24. Walmsley M, Cleaver D, Patient R. Fibroblast growth factor controls the timing of Scl, Lmo2, and Runx1 expression during embryonic blood development. *Blood*. 2008; 111:1157–1166.10.1182/blood-2007-03-081323 [PubMed: 17942750]
25. Songhet P, Adzic D, Reibe S, Rohr KB. fgf1 is required for normal differentiation of erythrocytes in zebrafish primitive hematopoiesis. *Developmental dynamics: an official publication of the American Association of Anatomists*. 2007; 236:633–643.10.1002/dvdy.21056 [PubMed: 17219402]
26. Yamauchi H, et al. Fgf21 is essential for haematopoiesis in zebrafish. *EMBO reports*. 2006; 7:649–654.10.1038/sj.embor.7400685 [PubMed: 16612391]
27. de Haan G, et al. In vitro generation of long-term repopulating hematopoietic stem cells by fibroblast growth factor-1. *Dev Cell*. 2003; 4:241–251. [PubMed: 12586067]
28. Yeoh JS, et al. Fibroblast growth factor-1 and -2 preserve long-term repopulating ability of hematopoietic stem cells in serum-free cultures. *Stem cells*. 2006; 24:1564–1572.10.1634/stemcells.2005-0439 [PubMed: 16527900]
29. Buono M, Visigalli I, Bergamasco R, Biffi A, Cosma MP. Sulfatase modifying factor 1-mediated fibroblast growth factor signaling primes hematopoietic multilineage development. *The Journal of experimental medicine*. 2010; 207:1647–1660.10.1084/jem.20091022 [PubMed: 20643830]
30. Zhao M, et al. FGF signaling facilitates postinjury recovery of mouse hematopoietic system. *Blood*. 2012; 120:1831–1842.10.1182/blood-2011-11-393991 [PubMed: 22802336]
31. Itkin T, et al. FGF-2 expands murine hematopoietic stem and progenitor cells via proliferation of stromal cells, c-Kit activation, and CXCL12 down-regulation. *Blood*. 2012; 120:1843–1855.10.1182/blood-2011-11-394692 [PubMed: 22645180]

32. Amaya E, Musci TJ, Kirschner MW. Expression of a dominant negative mutant of the FGF receptor disrupts mesoderm formation in *Xenopus* embryos. *Cell*. 1991; 66:257–270. [PubMed: 1649700]
33. Lee Y, Grill S, Sanchez A, Murphy-Ryan M, Poss KD. Fgf signaling instructs position-dependent growth rate during zebrafish fin regeneration. *Development*. 2005; 132:5173–5183.10.1242/dev.02101 [PubMed: 16251209]
34. Marques SR, Lee Y, Poss KD, Yelon D. Reiterative roles for FGF signaling in the establishment of size and proportion of the zebrafish heart. *Developmental biology*. 2008; 321:397–406.10.1016/j.ydbio.2008.06.033 [PubMed: 18639539]
35. Zhang C, Patient R, Liu F. Hematopoietic stem cell development and regulatory signaling in zebrafish. *Biochimica et biophysica acta*. 2013; 1830:2370–2374.10.1016/j.bbagen.2012.06.008 [PubMed: 22705943]
36. Hong CC, Peterson QP, Hong JY, Peterson RT. Artery/vein specification is governed by opposing phosphatidylinositol-3 kinase and MAP kinase/ERK signaling. *Current biology: CB*. 2006; 16:1366–1372.10.1016/j.cub.2006.05.046 [PubMed: 16824925]
37. Fouquet B, Weinstein BM, Serluca FC, Fishman MC. Vessel patterning in the embryo of the zebrafish: guidance by notochord. *Developmental biology*. 1997; 183:37–48.10.1006/dbio.1996.8495 [PubMed: 9119113]
38. Herbert SP, et al. Arterial-venous segregation by selective cell sprouting: an alternative mode of blood vessel formation. *Science*. 2009; 326:294–298.10.1126/science.1178577 [PubMed: 19815777]
39. Jin SW, Beis D, Mitchell T, Chen JN, Stainier DY. Cellular and molecular analyses of vascular tube and lumen formation in zebrafish. *Development*. 2005; 132:5199–5209.10.1242/dev.02087 [PubMed: 16251212]
40. Roehl H, Nusslein-Volhard C. Zebrafish *pea3* and *erm* are general targets of FGF8 signaling. *Current biology: CB*. 2001; 11:503–507. [PubMed: 11413000]
41. Bertrand JY, et al. Definitive hematopoiesis initiates through a committed erythromyeloid progenitor in the zebrafish embryo. *Development*. 2007; 134:4147–4156.10.1242/dev.012385 [PubMed: 17959717]
42. Iida A, et al. Metalloprotease-dependent onset of blood circulation in zebrafish. *Current biology: CB*. 2010; 20:1110–1116.10.1016/j.cub.2010.04.052 [PubMed: 20605457]
43. Murayama E, et al. Tracing hematopoietic precursor migration to successive hematopoietic organs during zebrafish development. *Immunity*. 2006; 25:963–975.10.1016/j.immuni.2006.10.015 [PubMed: 17157041]
44. Jin H, Xu J, Wen Z. Migratory path of definitive hematopoietic stem/progenitor cells during zebrafish development. *Blood*. 2007; 109:5208–5214.10.1182/blood-2007-01-069005 [PubMed: 17327398]
45. Kissa K, et al. Live imaging of emerging hematopoietic stem cells and early thymus colonization. *Blood*. 2008; 111:1147–1156.10.1182/blood-2007-07-099499 [PubMed: 17934068]
46. Itoh N. The Fgf families in humans, mice, and zebrafish: their evolutionary processes and roles in development, metabolism, and disease. *Biological & pharmaceutical bulletin*. 2007; 30:1819–1825. [PubMed: 17917244]
47. Thisse B, et al. Spatial and temporal expression of the zebrafish genome by large-scale in situ hybridization screening. *Methods in cell biology*. 2004; 77:505–519. [PubMed: 15602929]
48. Lawson ND, et al. Notch signaling is required for arterial-venous differentiation during embryonic vascular development. *Development*. 2001; 128:3675–3683. [PubMed: 11585794]
49. Bigas A, D’Altri T, Espinosa L. The Notch pathway in hematopoietic stem cells. *Current topics in microbiology and immunology*. 2012; 360:1–18.10.1007/82\_2012\_229 [PubMed: 22692832]
50. You LR, et al. Suppression of Notch signalling by the COUP-TFII transcription factor regulates vein identity. *Nature*. 2005; 435:98–104.10.1038/nature03511 [PubMed: 15875024]
51. Szeto DP, Griffin KJ, Kimelman D. HrT is required for cardiovascular development in zebrafish. *Development*. 2002; 129:5093–5101. [PubMed: 12397116]

52. Walsh DW, Godson C, Brazil DP, Martin F. Extracellular BMP-antagonist regulation in development and disease: tied up in knots. *Trends in cell biology*. 2010; 20:244–256.10.1016/j.tcb.2010.01.008 [PubMed: 20188563]
53. Furthauer M, Thisse B, Thisse C. Three different noggin genes antagonize the activity of bone morphogenetic proteins in the zebrafish embryo. *Developmental biology*. 1999; 214:181–196.10.1006/dbio.1999.9401 [PubMed: 10491267]
54. Nicoli S, Gilardelli CN, Pozzoli O, Presta M, Cotelli F. Regulated expression pattern of gremlin during zebrafish development. *Gene expression patterns: GEP*. 2005; 5:539–544.10.1016/j.modgep.2004.11.001 [PubMed: 15749084]
55. Lieschke GJ, et al. Zebrafish SPI-1 (PU.1) marks a site of myeloid development independent of primitive erythropoiesis: implications for axial patterning. *Developmental biology*. 2002; 246:274–295.10.1006/dbio.2002.0657 [PubMed: 12051816]
56. Korchynskiy O, ten Dijke P. Identification and functional characterization of distinct critically important bone morphogenetic protein-specific response elements in the Id1 promoter. *The Journal of biological chemistry*. 2002; 277:4883–4891.10.1074/jbc.M111023200 [PubMed: 11729207]
57. Jankovic V, et al. Id1 restrains myeloid commitment, maintaining the self-renewal capacity of hematopoietic stem cells. *Proceedings of the National Academy of Sciences of the United States of America*. 2007; 104:1260–1265.10.1073/pnas.0607894104 [PubMed: 17227850]
58. Row RH, Kimelman D. Bmp inhibition is necessary for post-gastrulation patterning and morphogenesis of the zebrafish tailbud. *Developmental biology*. 2009; 329:55–63.10.1016/j.ydbio.2009.02.016 [PubMed: 19236859]
59. Siekmann AF, Covassin L, Lawson ND. Modulation of VEGF signalling output by the Notch pathway. *BioEssays: news and reviews in molecular, cellular and developmental biology*. 2008; 30:303–313.10.1002/bies.20736
60. Marshall CJ, Kinnon C, Thrasher AJ. Polarized expression of bone morphogenetic protein-4 in the human aorta-gonad-mesonephros region. *Blood*. 2000; 96:1591–1593. [PubMed: 10942412]
61. de Bruijn MF, et al. Hematopoietic stem cells localize to the endothelial cell layer in the midgestation mouse aorta. *Immunity*. 2002; 16:673–683. [PubMed: 12049719]
62. Taoudi S, Medvinsky A. Functional identification of the hematopoietic stem cell niche in the ventral domain of the embryonic dorsal aorta. *Proceedings of the National Academy of Sciences of the United States of America*. 2007; 104:9399–9403.10.1073/pnas.0700984104 [PubMed: 17517650]
63. Wilkie AO, Patey SJ, Kan SH, van den Ouweland AM, Hamel BC. FGFs, their receptors, and human limb malformations: clinical and molecular correlations. *American journal of medical genetics*. 2002; 112:266–278.10.1002/ajmg.10775 [PubMed: 12357470]
64. Ueno H, Gunn M, Dell K, Tseng A Jr, Williams L. A truncated form of fibroblast growth factor receptor 1 inhibits signal transduction by multiple types of fibroblast growth factor receptor. *The Journal of biological chemistry*. 1992; 267:1470–1476. [PubMed: 1309784]
65. Tonou-Fujimori N, et al. Expression of the FGF receptor 2 gene (fgfr2) during embryogenesis in the zebrafish *Danio rerio*. *Mechanisms of development*. 2002; 119 (Suppl 1):S173–178. [PubMed: 14516681]
66. Groves JA, Hammond CL, Hughes SM. Fgf8 drives myogenic progression of a novel lateral fast muscle fibre population in zebrafish. *Development*. 2005; 132:4211–4222.10.1242/dev.01958 [PubMed: 16120642]
67. Pyati UJ, Webb AE, Kimelman D. Transgenic zebrafish reveal stage-specific roles for Bmp signaling in ventral and posterior mesoderm development. *Development*. 2005; 132:2333–2343.10.1242/dev.01806 [PubMed: 15829520]
68. Westerfield, M. *The Zebrafish Book; A Guide for the Laboratory Use of Zebrafish (Brachydanio rerio)*. 2. University of Oregon Press; Eugene: 1993. 300P (Book)
69. Gonzalez-Quevedo R, Lee Y, Poss KD, Wilkinson DG. Neuronal regulation of the spatial patterning of neurogenesis. *Dev Cell*. 2010; 18:136–147.10.1016/j.devcel.2009.11.010 [PubMed: 20152184]



70. Sacilotto N, et al. Analysis of Dll4 regulation reveals a combinatorial role for Sox and Notch in arterial development. *Proceedings of the National Academy of Sciences of the United States of America*. 2013; 110:11893–11898.10.1073/pnas.1300805110 [PubMed: 23818617]

Author Manuscript

Author Manuscript

Author Manuscript

Author Manuscript

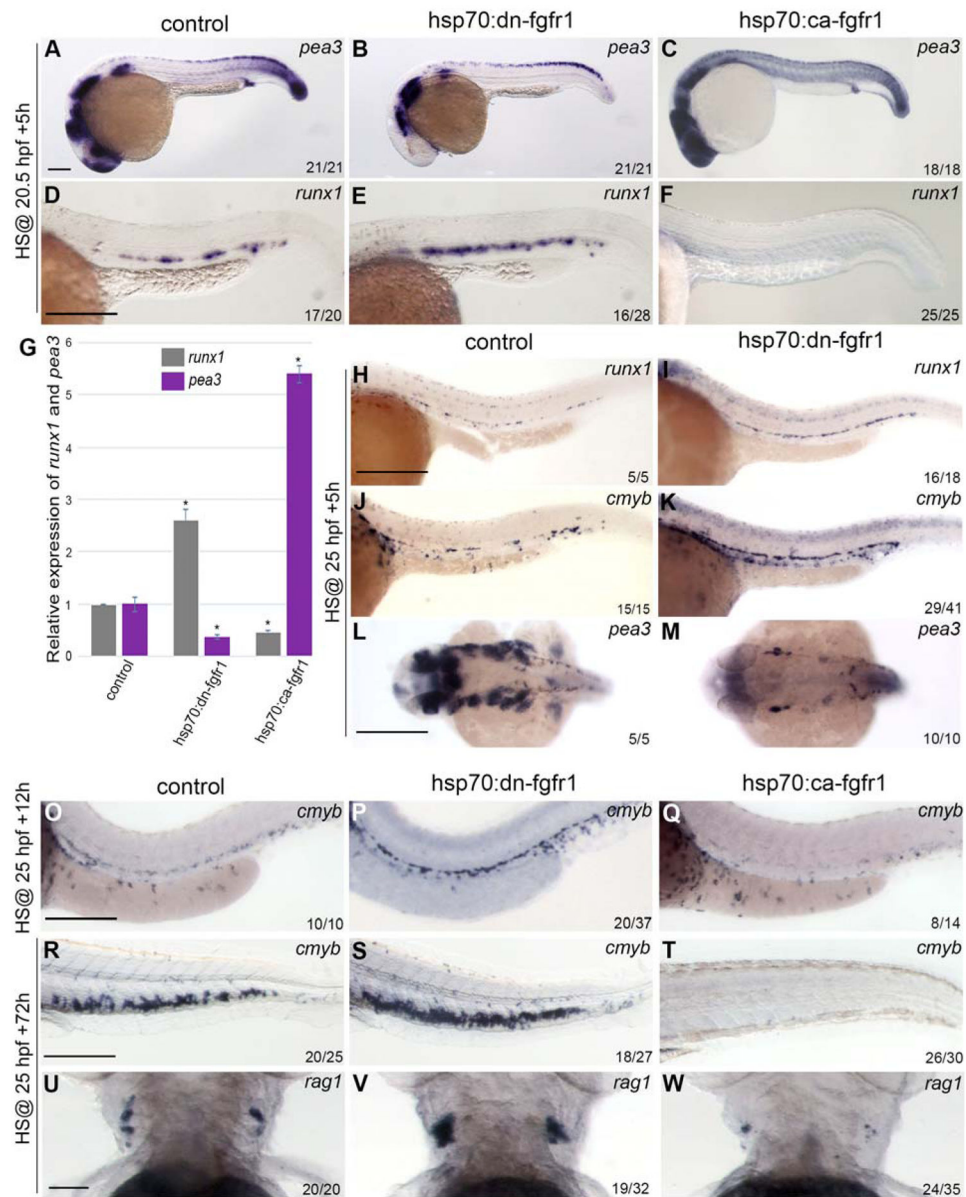


**Figure 1. FGF signaling represses HSC formation and maintenance**  
 (A–F) Embryos were heatshocked at 20.5 hpf and analyzed at 26 hpf. (A–C) *pea3* expression is downregulated in *hsp:dn-fgfr1* (B) and upregulated in *hsp70:ca-fgfr1* embryos (C) compared to controls (A). (D–F) Aortic expression of *runx1* is enhanced in *hsp70:dn-fgfr1* (E) and depleted in *hsp70:ca-fgfr1* embryos (F) compared to controls (D). (G) Quantification of *runx1* and *pea3* mRNA expression in dissected trunks normalized to *ef1a*. Expression of each gene was set to 1 in the control. Data are shown as average  $\pm$  s.d. values;  $p < 0.001$ . (H–M) Embryos were heatshocked at 25 hpf and analyzed at 30 hpf. (H–I) *runx1* expression is increased in *hsp70:dn-fgfr1* embryos (I) compared with controls (H). Similar results are seen with *cmyb* expression in control (J) and *hsp70:dn-fgfr1* embryos (K). (L and M) Dorsal view of *pea3* expression in the head shows downregulation of *pea3* upon depletion of FGF signaling. (O–W) Embryos were heatshocked at 25hpf and analyzed 12h

and 72hphs. (O–Q) *cmyb* expression is more intense in the *hsp70:dn-fgfr1* embryos (P) compared to control embryos (O). Conversely, embryos in which FGF signaling is increased, display a drastic diminution of *cmyb* expression (Q). (R–S) Comparison of *cmyb* expression in the CHT of heatshocked transgenic embryos and controls. The augmentation of HSC numbers detected at 26hpf upon FGF modulation is maintained in the CHT of the *hsp70:dn-fgfr1* embryos while the CHT of the *hsp70:ca-fgfr1* embryos are devoid of *cmyb* cells. (U–W) Effect of FGF signal alteration on T-cells. FGF ablation (V) or augmentation (W) has opposite effects on *rag1+* cells. Scale bars: (A) 50um, (D, H) 200um, (L, O, R) 250um, (U) 50um.

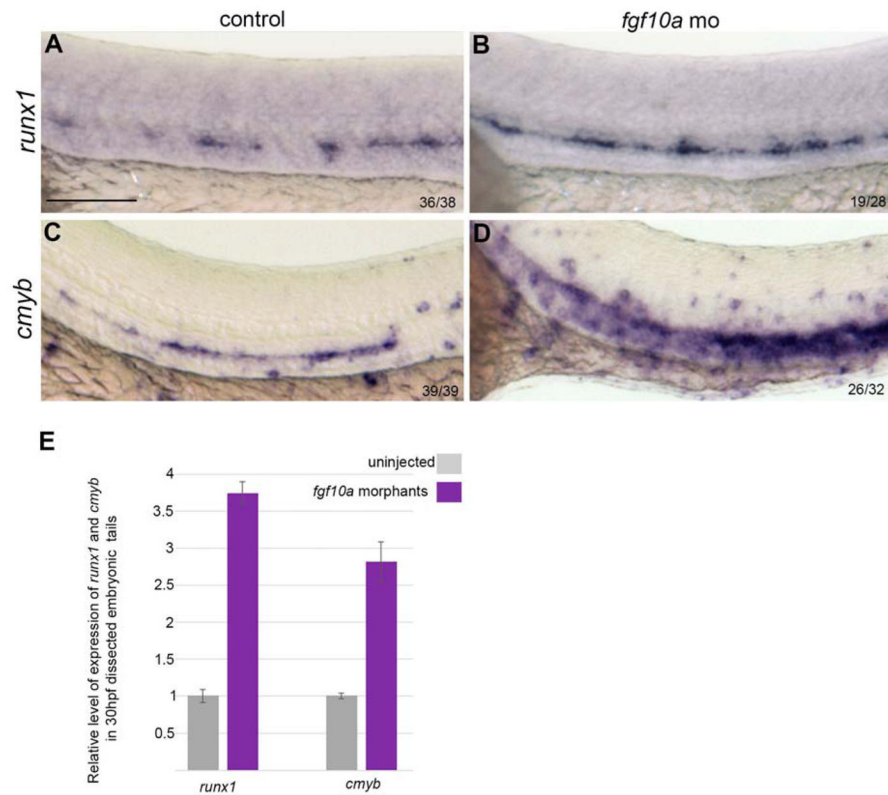


**Figure 2. Loss of *fgf10a* mimics the effect of FGF ablation**  
 (A–B) *runx1* expression is expanded along the entire DA in the morphant embryos.  
 Similarly, loss of Fgf10a significantly increases *cmyb* expression in the aortic region (C–D).  
 Comparison of the relative level of expression of *runx1* and *cmyb* by qPCR in control and morphant embryos (E). Scale bar: 150um.

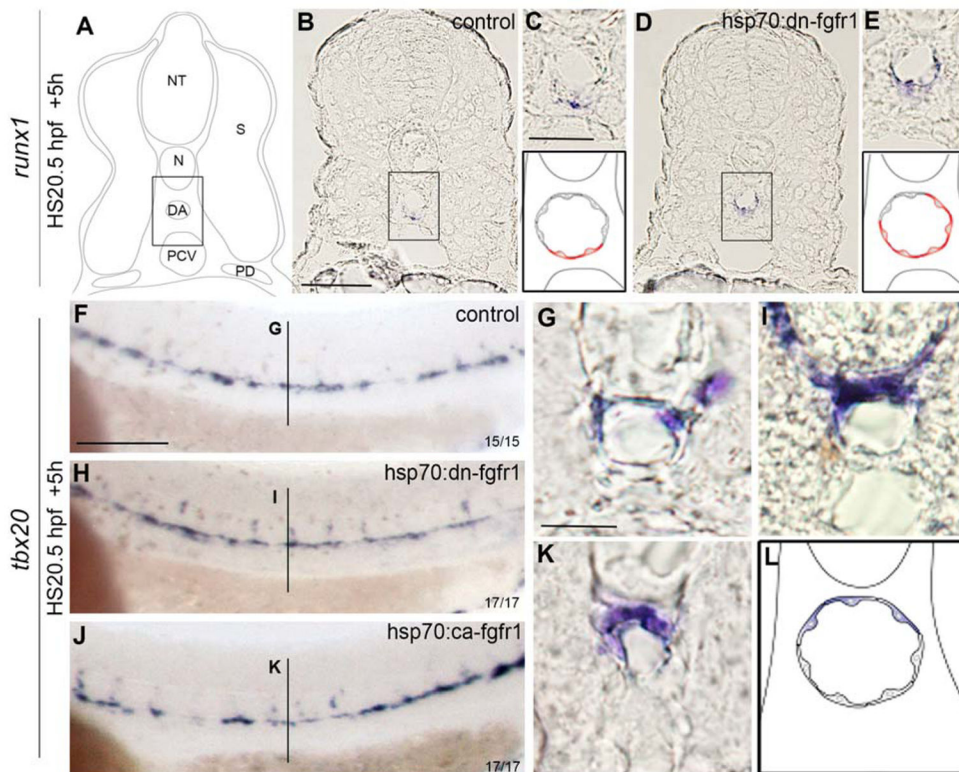


**Figure 3. Loss of FGF signaling expands *runx1* dorsally without affecting dorsal polarization of the DA**

(A) Schematic representation of a trunk section of 26hpf embryos. (B) Aortic localization of *runx1*<sup>+</sup> cells in control (B and C) and *hsp70:dn-fgfr1* (D and E) embryos. Expression of *tbx20* in control (F and G), *hsp70:dn-fgfr1* (H and I), and *hsp70:ca-fgfr1* (J and K) embryos. The black line (G, I and K) denotes where sections were made. (L) Schematic representation of *tbx20* expression in the roof of the DA. DA: dorsal aorta, N: notochord, NT: neural tube, PCV: posterior cardinal vein; PD: pronephric duct, S: somite. Scale bars: (B) 30um, (F) 200um, (G) 20um.

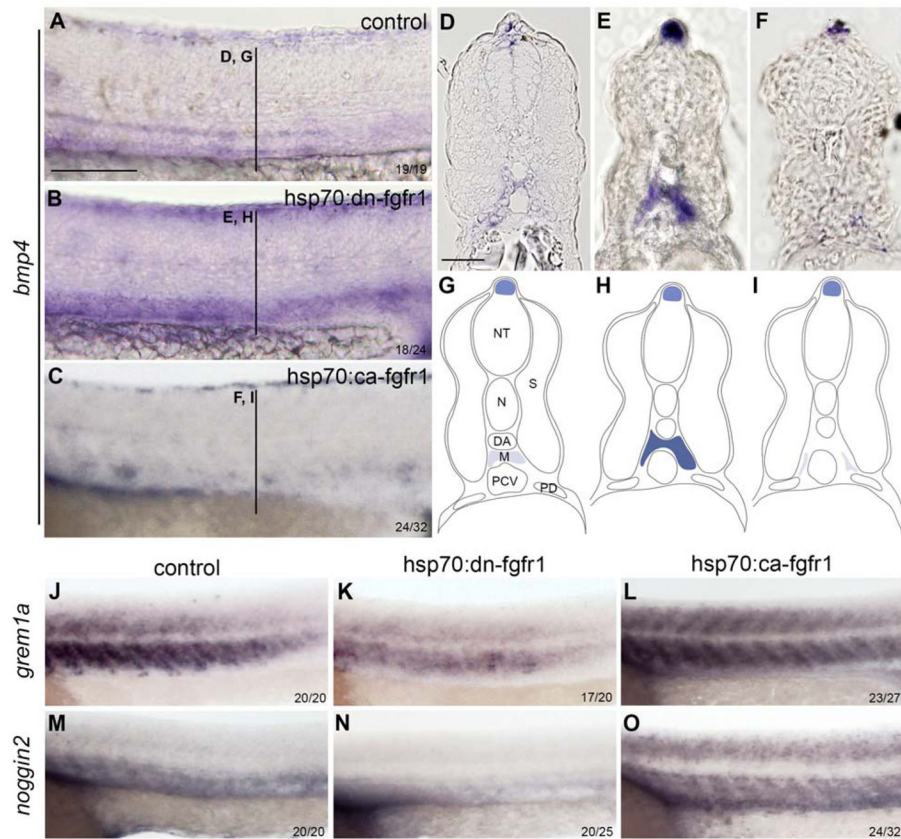


**Figure 4. FGF signaling regulates *Bmp4* expression, as well as *noggin2* and *gremlin1a*, two BMP antagonists**

(A–C) *bmp4* expression is altered following manipulation of FGF signaling. *bmp4* levels of expression are increased in *hsp70:dn-fgfr1* embryos (B and E) and decreased in *hsp70:ca-fgfr1* embryos (C and F). (D–F) Transverse sections of embryos from WISH samples (A–C). (G–I) Schematic representing *bmp4* expression in control (G), *hsp70:dn-fgfr1* (H), and *hsp70:ca-fgfr1* (I) embryos. (J–O) *gremlin1a* (J–L) and *noggin2* (M–O) expression is reduced in *hsp70:dn-fgfr1* embryos (K and N), and enhanced in *hsp70:ca-fgfr1* embryos (L and O). M: mesenchyme. Scale bars: (A) 200um, (D) 50um.

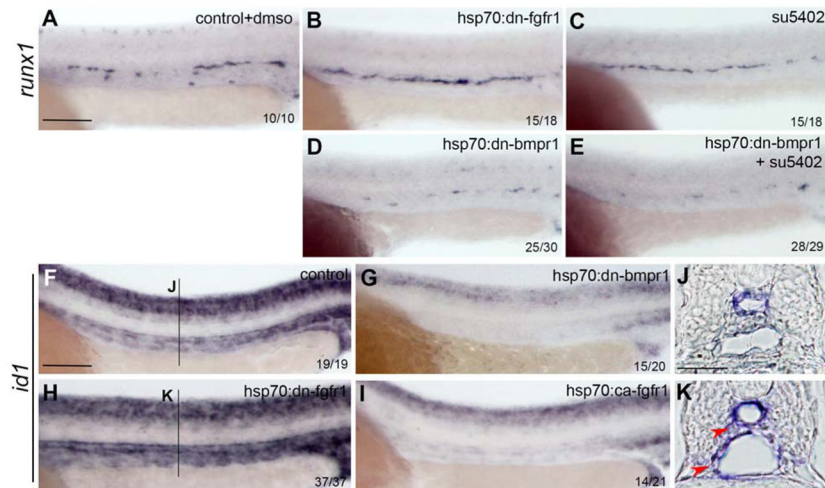


### Figure 5. Epistatic analysis of BMP and FGF signaling interaction

(A–C) *runx1* expression is increased in *hsp70:dn-fgfr1* embryos (B) and embryos treated with su5402 (C) compared to controls (A). Overexpression of *hsp70:dn-bmpr1* impairs emergence of HSCs (D) compared to control (A) or FGF inhibited embryos (B and C). HSC emergence is not rescued in *hsp70:dn-bmpr1* embryos following blockade of FGF signaling using su5402 (E). (F–P) *id1* expression is reduced upon inhibition of BMP signaling (G) as well as augmentation of FGF signaling (K), compared to control embryos (F). In the absence of FGF signaling, *id1* expression is increased in the vasculature and in some cells surrounding the vessels (N, and K, red arrows). Scale bars: (A, F) 100um, (J) 30um.

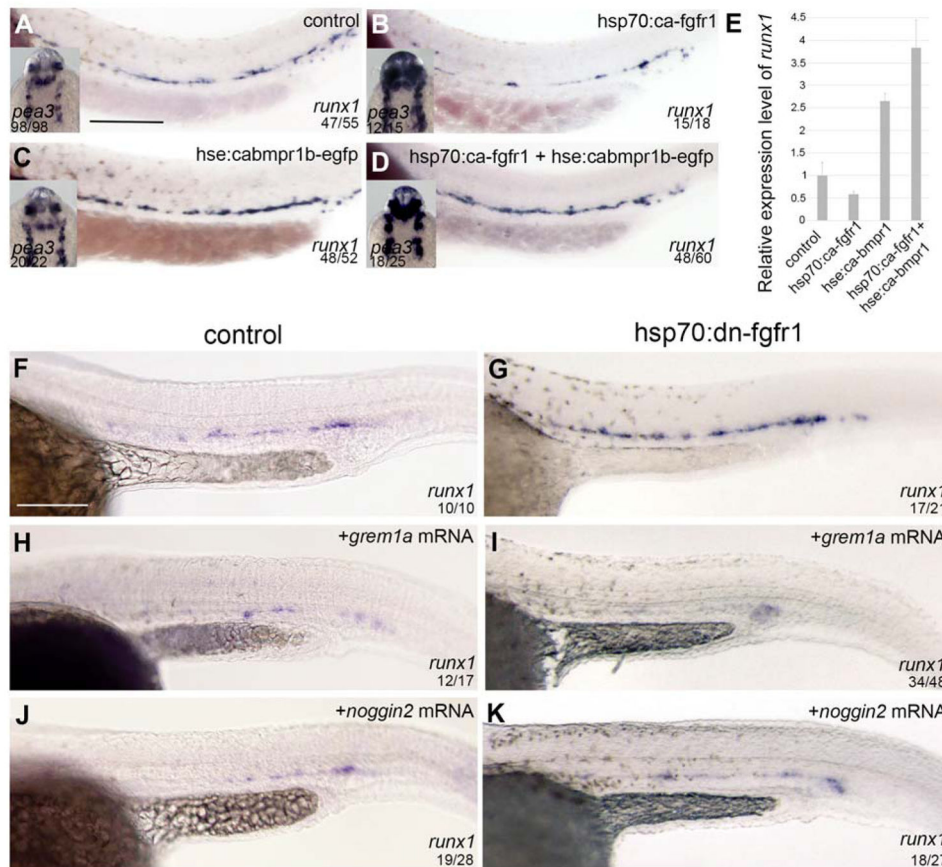


**Figure 6. Ectopic activation of BMP signaling rescues *runx1* expression in an activated FGF background**

(A–D) *runx1* expression increases in the DA following activation of the BMP pathway (C), compared to controls (A). *runx1* expression in *hsp70:ca-fgfr1* (B) embryos is rescued by activation of a *hse:cabmpr1b* transgene (D). Quantitative analysis of *runx1* expression (E). *pea3* expression in the head (inserts, A–D) is upregulated upon FGF activation. (F–K) *runx1* expression is impaired upon overexpression of either *gremlin1a* (H) or *noggin2* (J) compared to control (F). Inhibition of FGF signaling fails to rescue *runx1* expression when *gremlin1a* (I) and *noggin2* (K) are overexpressed. Scale bars: (A, F) 200µm.



